Visual Landmark Constellation matching for spacecraft pinpoint landing

Bach Van Pham* , Simon Lacroix† and Michel Devy‡
LAAS-CNRS, University of Toulouse, 7 Avenue du Colonel Roche, Toulouse Cedex 4, 31077, France
Marc Drieux§
EADS-ASTRIUM, 66 Route de Verneuil, Les Mureaux Cedex , 78133, France
Christian Phillipe¶
ESTEC/ESA, Keplerlaan 1 , Postbus 299 , 2200 AG Noordwijk , The Netherlands

This paper presents a vision-based approach to estimate the absolute position of a planetary lander during the last stages of the descent. The approach relies on the matching of landmarks detected in the descent imagery with landmarks previously detected in orbiter images. The matching process must be robust with respect to scale and radiometry differences in the image data: it mainly relies on the geometric repartition of the landmarks, rather than on radiometric signatures computed from the image signal. It must also satisfy other requirements like low memory requirement and efficient hardware implementation due to spatial system's constraints. First results using a simulator are presented and discussed.

Nomenclature

H, h	Spacecraft or obiter's height
M, m	Image's sizes
F, f	Camera's field of view
R, r	Image's resolution
s	Scale difference
br	Inner circle's radius
pr	Outer circle's radius
D	Pixelics distance
$nRings$	Number of rings
$nWedges$	Number of wedges (sectors)
p	Landmark's signature
L, K	Landmarks
P	Landmark's warped position
δ	Landmarks minimum distance
$distVector$	Vector distance
ε	Vector distance threshold
AF	Affine Transformation
U	Image's 2D position
M	Surface's 3D position
K	Camera's intrinsic matrix
R	Camera's image rotation matrix

*PhD Student, Group Robotics and Interactive Systems
†Research Scientist, Group Robotics and Interactive Systems
‡Research Scientist, Group Robotics, Action and Perception
§Sensors engineering and Image processing Enginneer
¶Head of Guidance, Navigation and Control Section

T	Camera's image translation matrix
Subscript	
i, j	Variable number

I. Introduction

Planetary exploration missions may require a precise landing position, in order to avoid obstacles or to get close to scientifically interesting areas assessed on the basis of orbiter images. However, current Entry, Descent and Landing (EDL) techniques are still far from this capability. Hence, much of research has been conducted in the field of absolute localization (referred to as "pinpoint landing"),[3,5,7,11,12] which allows the spacecraft to localize itself with respect to a known reference and navigate to a pre-defined landing site.

I.A. Related Work

Various technologies for absolute localization with respect to initial data for aerial devices have been developed for military purposes (cruise missiles). Such technologies have been modified to safely land a spacecraft on a pre-defined spot on extraterrestrial planets. For example, in the Vision aided inertial navigation (VISINAV) system:[11] surface landmarks in the descent images are extracted and matched to an ortho-rectified image of the scene that is registered with a digital elevation map. The mapped landmarks returned by this process are then used either to estimate or update the spacecraft position. In parallel with these mapped landmarks, the VISINAV system employs the persistent features to track mapped landmarks through a sequence of descent images to estimate the global position of the spacecraft, and the opportunistic features to estimate the spacecraft five degree-of-freedom motion. These estimations along with the IMU measurements are then provided to an Extended Kalman Filter to update the spacecraft status. A main drawback of this system is its high memory requirement due to the usage of image correlation in finding mapped landmarks. In fact, the whole system must store in its memory the concerned map (or at least several high contrast regions in the whole map) and the associated 3D data, which is memory costful.

Another pinpoint landing system[3] uses craters for precise position estimation. Craters are excellent landmarks for the system thanks to their illumination, scale and rotation invariance properties. The crater shapes commonly follow a known geometric model (ellipse), invariant to scale changes and orientation between the spacecraft camera and the surface. Naturally, areas with either too few or too many craters challenge such an approach. Difficulties also arise in regions with blur rimmed, broken, overlapped or overshadowed (with low sun's elevation) craters.

In another article,[12] a pinpoint landing system which uses SIFT features (Scale Invariant Feature Transform)[8] as mapped landmark to estimate the spacecraft's global position is proposed. SIFT detector converts interest points in both the descent image and the geo-referenced orbiter image into feature vectors, which are later matched to each other. Unlike craters, SIFT does not rely on a known model of terrain shape but on the image texture. It neither requires an IMU nor an altimeter like VISINAV to find mapped landmarks. SIFT features are also well-known for their scale invariance properties. However, they are only invariant to an affine transformation in illumination change. Thus, they are quite vulnerable in case of important illumination changes between the orbiter and descent images, such as caused by the difference of the suns direction.

Another method[5] relying on a Lidar sensor and the matching of landmark constellations (star tracker like method) is also proposed. Firstly, surface landmarks, which are either maximum/minimum of the surface's height and slope, are extracted from the surface elevation image provided by the Lidar sensor. The metric distances of one landmark with its neighbors are used as its signature. Surface and DEM (digital elevation map) landmarks matching is performed by comparing the landmark's signature with those of the map. The main drawback of this system is its hardware requirement. In fact, this system requires that the resolution of the surface image obtained with the Lidar sensor must be equivalent to that of the map image. That means the sensor's field of view must be adaptively changed with the spacecraft's speed and altitude to have equal surface sampling step. Other pinpoint landing techniques can be found in the overview article of A. E. Johnson et al.[7]

The absolute positioning system Landstel (Landmark Constellation) introduced in this paper is designed to cope with several constraints like low memory requirement, hardware implementation facility and illumi-

nation change robustness. This Landstel system uses camera as its primary sensor, along with an altimeter and an inertial sensor, with which the lander always equips. The main features used by the Landstel system is the image's corners like Harris corner points.[6] The assumption used by this system is that image's corners which also represent surface's corners are not very sensitive to illumination changes in term of geometric location. For example, the top of a rock piece is always revealed as a corner and is slightly moved around given different illumination conditions even though its radiometric value in the associated images can be greatly modified. As the Landstel system only uses image's features to estimate the spacecraft's position, it is therefore more efficient in term of memory than other systems which use image correlation since it does not have to store the whole landing map like the others. Similarly to the Lidar based pinpoint landing approach[5] mentionned above, the Landstel system also uses the relationship of one landmark with its neighbors as its signature.

I.B. Paper outline

The next section sketches the overall architecture in which the Landstel system is integrated, and presents various steps of the Landstel landmark matching algorithm. Due to the complexity of the whole navigation system, this paper only presents the mechanism and results obtained with the Landstel system, which provides spacecraft's absolute position estimation. The issue of fusing this position estimate with other navigation sources (IMU and visual landmark tracking) is not considered in this paper. The main steps of the Landstel system are depicted in Section III. Some matching results obtained in simulation with PANGU[9] are also presented in this section. Section IV briefly explains how the spacecrafts absolute position can be estimated with matched landmarks. Section V and VI then respectively discuss the approach and conclude the paper.

II. OVERALL SYSTEM DESCRIPTION

Figure 1 presents the overall navigation system architecture. The Landstel system is composed of one off-line and one on-line part. In the off-line part, the Digital Elevation Map and the associated 2D ortho-image of the foreseen landing area ($30km \times 30km$ for the current technology[13]) is obtained on the basis of orbiter imagery (this process being naturally out of the scope of our system). Visual landmarks (initial landmarks) are then extracted in the ortho-image, using the Harris feature points detector.[6] Depending on the nature of the landing terrain, the appropriate visual landmarks are chosen. A signature is defined for each of the extracted feature points, according to the process introduced in section III.C. The initial landmarks 2D position, their signature and their 3D absolute co-ordinates on the surface constitute a database that is stored in the landers memory.

On-line: the current altitude estimate is exploited to extract landmarks (denoted as persistent landmarks), and the current spacecraft orientation estimate is used to warp the landmark coordinates, so as to enable matches with initial landmarks. Then, spacecraft's absolute position estimated from these matches and other information like spacecraft's speed, orientation, previous absolute position estimation are then fused to re-estimate the spacecraft's absolute position. In the remainder of the paper, the terms geo-referenced image and orbiter image are interchangeably used similarly, the terms landing image and spacecraft image denote the same image.

III. MAPPED LANDMARK MATCHING

III.A. Landmark Detection

Unlike the landmark extraction method used for the geo-referenced image, which is purely a Harris operator, the landmarks of the landing image are extracted with a scale adjustment operator.[4] With the use of an altimeter, the system can detect the difference between scales of the geo-referenced image and the landing one. Similarly to the scale notion introduced by Dufournaud et al.,[4] which is the fraction between the resolutions of two images with the same image's sizes and taken by the same camera, the scale notion we used here is its expansion, applied for two images obtained with two different cameras.

Given (M, M) the size of a square 2D ortho geo-referenced image, H its altitude and F its camera's field

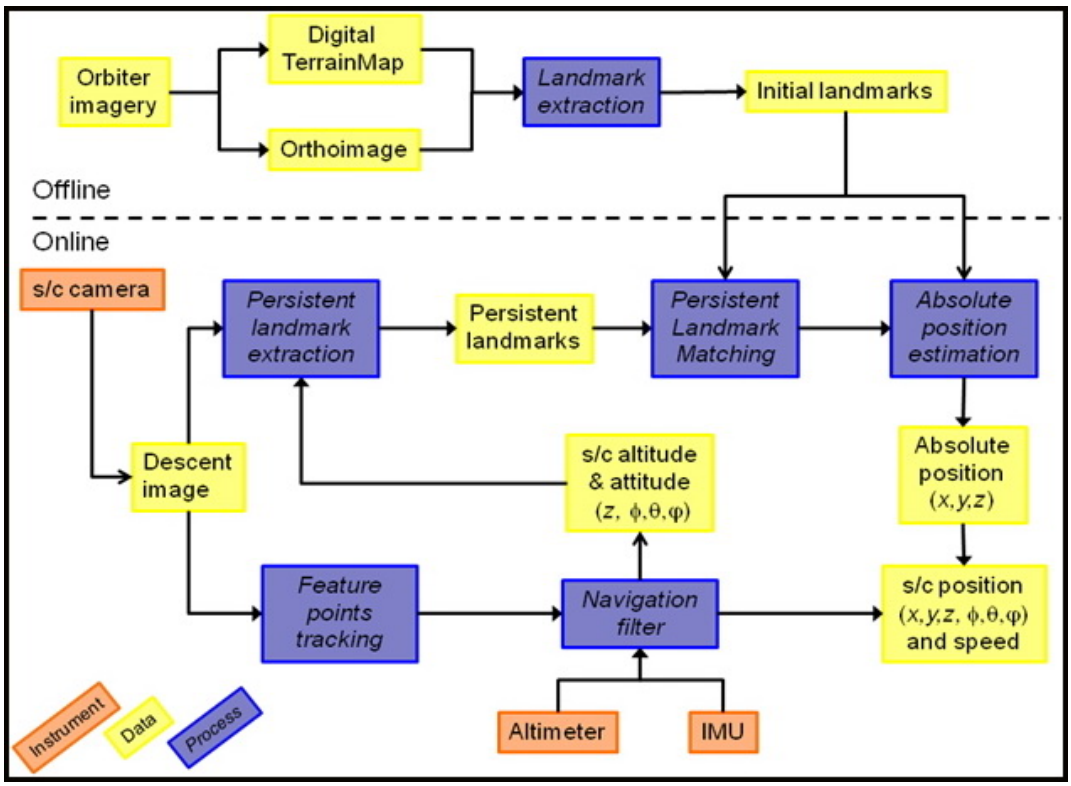

Figure 1. Overall System Architecture. The feature point tracking and navigation filter processes are no further described in this paper. The navigation filter process is only sketched here to exhibit its interfaces with the Landstel system (highlighted in blue in the figure): current altitude and attitude estimates are used to assist the landmark matching process, whereas the output of the Landstel system (translation components of the spacecraft absolute position) is fused with the altimeter, IMU and feature tracking processes to produce a global spacecraft position estimate.

of view, the geo-referenced image's resolution can be calculated with:

$$R = \frac{Htan(\frac{F}{2})}{2M}(m/pixel) \tag{1}$$

similarly, with (m, m) the size of the landing image, h its altitude obtained with the altimeter and f its camera's field of view, supposing that the camera points nadir, then the landing image's resolution is:

$$r = \frac{htan(\frac{f}{2})}{2m}(m/pixel) \tag{2}$$

The scale difference between the two images is:

$$s = \frac{R}{r} \tag{3}$$

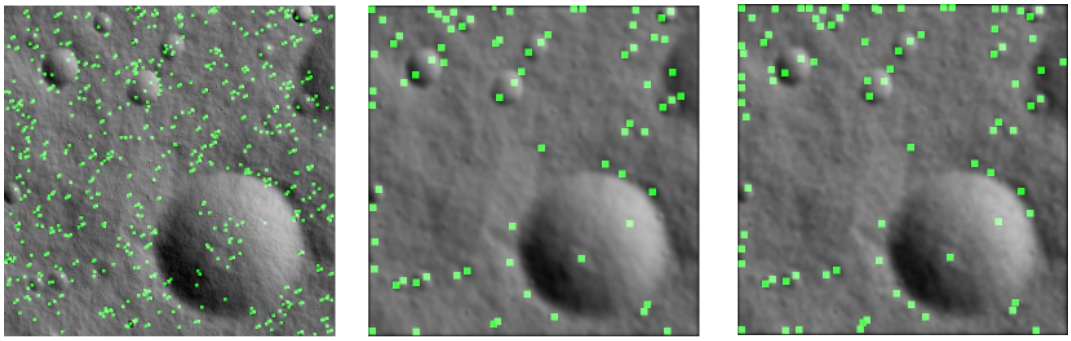

Figure 2. Landmarks Detection with Scale Adjustment Operator (a) Normal operator (b) Scale Adjustment Operator (c) Scale Adjustment Operator with Noise

As stated in an article of Dufournaud et al.,[4] the scale-space associated with an image I can be obtained by convolving the initial image with a Gaussian kernel whose standard deviation is increasing monotonically, say $s\sigma$ with $s > 1$. In figure 2, the landmarks which are visible at high altitude are detected in figure 2.b ($\sigma = 3$), and the landmarks which are invisible at high altitude (shown in figure 2.a) are discarded in figure 2.b. The Landstel system, in addition, uses the scale-space pyramid like for the SIFT detection method[8] to compensate the altimeters error. However, the Landstel landmark detector is less costly than SIFT since it does not calculate the SIFT descriptor.

The usage of scale adjustment operator, on one hand, helps to remove landmarks in the landing image that have not been extracted in the geo-referenced image. On the other hand, it filters the sensor noise thanks to the use of Gaussian kernel. Figure 2.c shows landmarks detected in an image altered by white noise $(0, 0.01)$ with $\sigma = 4$.

III.B. Landmark Rectification

Once they have been extracted from the spacecrafts image with the scale adjustment operator, the interest points are warped to match the orbiters image's orientation with a homography transformation (figure 3.left), estimated thanks to the spacecraft orientation provided by the navigation filter. In fact, during this step, the landing zone is considered as a flat area due to the long distance between the spacecraft and the surface. This step will naturally ease the landmark matching process. Figure 3.right shows that the detected landmarks are pretty well matching with those of the geo-referenced image thanks to the usage of the scale adjustment operator and the image warping.

III.C. Landmark Signature Extraction

Thanks to the scale adjustment, the detected landmarks have a pixel metric resolution similar to that of landmarks in the orbiters image. The Landstel system uses this property to find matches between landmarks

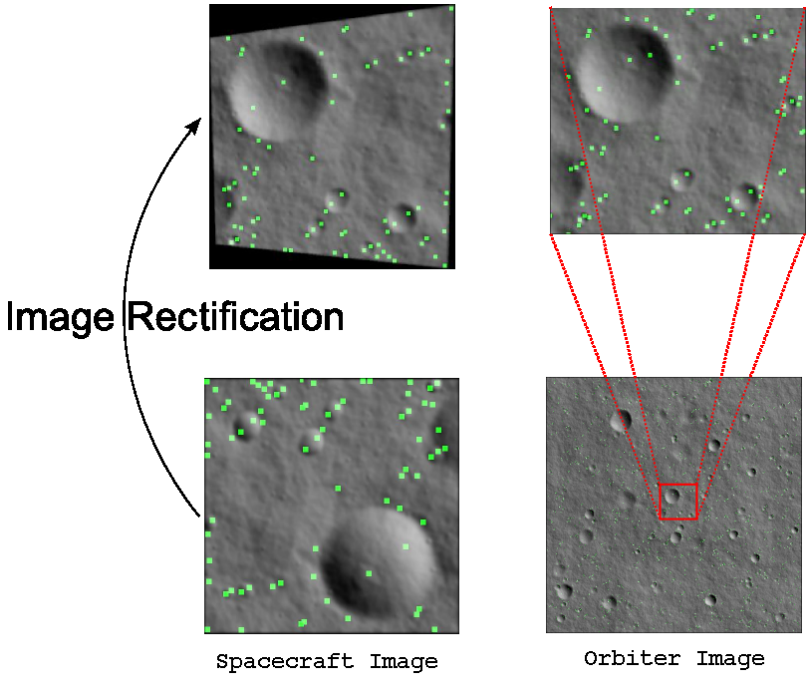

Figure 3. (a) Rectification of spacecraft image (b) Corresponding zoomed region in geo-referenced image

extracted from these two images: the signature the landmark is indeed defined using their relative geometric repartition, measured using the Shape Context algorithm.[2]

For a landmark L_i, its signature is extracted by using the Shape Context algorithm basing on the pixelic distance, which is composed of the following steps:

1. *Determination of Neighbors set*: a generic landmark L_j can be added to the Neighbors set of L_i if and only if its pixelic distance to L_i, D_{ij}, satisfies the following condition

$$br < D_{ij} < pr \tag{4}$$

   where br is the minimum distance which is used to prevent noise and pr is the pattern radius (figures 4.a and 4.b, extracted from[10]).

2. *Angular Distances Discretization and Sector Discretization*: the landmarks pixelic distances and their angular values in the Neighbors set of L_i are then discretized into a bi-dimensional $nRings \times nWedges$ values, corresponding to $nRings$ rings centered on L_i and to $nWedges$ sectors. The signature is then normalized into a probabilistic distribution.

Therefore, for a landmark, its signature is a bi-dimensional vector of $nRings \times nWedges$ bytes.

Notes:

1. In this algorithm, the use of the inner radius br is to avoid noise generated in the landing images landmarks. Let δ the minimum distance between two landmarks, which is defined for both geo-referenced lander images. In the Landstel system, the minimum distance δ' of two rectified landmarks will be smaller than δ. Therefore, br will be used to reject those rectified landmarks which are too near to the current landmark L_i.

2. The value of pr is chosen considering the rectified images size of the last image in the test sequence. For example, the last image of the first experimental series (section IV) is acquired at $3200m$ altitude. And its rectified image will have approximately 286×286 pixels. In this case, pr is assigned to 100, which is used for the whole series. In reality, the value of pr depends on the pyramid model of the geo-referenced images.

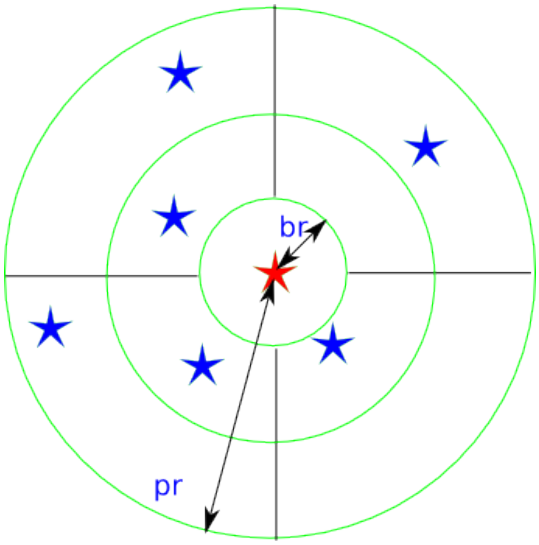

Figure 4. The principle of the Shape Context algorithm

3. The value of $nRings$ (number of Rings) and $nWedges$ (number of sectors) depend on the uncertainty of the landmarks position, which is influenced by the noise on the image and the attitude.

III.D. Landmarks Matching

In order to calculate the similarity between two landmarks, the Chi-Square distance between the two landmarks signatures is calculated:

$$C_{gh} = \frac{1}{2}\sum_{k=1}^{k}\frac{[g(k)-h(k)]^2}{g(k)+h(k)} \tag{5}$$

where C_{gk} is the Chi-Square distance between two features g and k.

The couple whose distance is smaller than a threshold is considered as a potential match. Therefore, each landmark L_i in the landing image may have multiple possible matches. During this step, the spacecrafts landmarks and their corresponding possible matches are memorized in a data structure, called $matchIndex$.

III.E. Multiple hypothesis matches removal

The multiple possible matches found in the previous steps are filtered out with the Multiple hypothesis matches removal procedure. The main idea of this procedure is that two corresponding sets of matched points must represent the same constellation (similarly to the case of star tracker). Therefore, the system will firstly find a set of 5 consistent matches. The search of these consistent matches is based on the vector distance. Given two couples (L_i, K_i) and (L_j, K_j) where L and K respectively represent the spacecrafts and orbiters landmarks, these two matches are considered as consistent if and only if their vector distance $distVector([L_i, L_j], [K_i, K_j])$, defined as the difference between the two vectors lengths and orientations, is smaller than a predefined threshold ε. This vector distance is meaningful because the two landmark sets share the same coordinate system. Therefore, the only unknown factor is the translation value of the two sets.

The *Multiple hypothesis matches removal* procedure encompasses the following steps:

1. Find at least 5 consistent matches between the spacecrafts landmarks and the orbiters landmarks using the vector distance. If the system cannot find at least 5 consistent matches, it will report a failure.

2. After having found 5 consistent matches, the affine transformation AF between the spacecrafts rectified landmarks and the orbiters landmarks is calculated.

3. Apply the AF transformation calculated to every spacecrafts rectified landmarks. The result of each transformation is compared with the orbiters landmarks. The couple which is consistent in orbiters pixelic position is retained as a match, which means that their difference in position is smaller than ε.

The *Multiple hypothesis matches removal* can be described with the following pseudo code:

Let $mMatchIndexSize$ the size of $matchIndex$.

1. Set $mResult = 0$; $mMatch = NULL$;
2. For $i = 1 : mMatchIndexSize$ - 4
   a. Get landmark L_i in $matchIndex$
   b. Set $nCouple = 0$;
   c. For each possible match of L_i (let K_i the current possible match)
      i. For $j = i + 1 : mMatchIndexSize$
         1. Get landmarks L_j in $matchIndex$
         2. For each possible match of L_j (let K_j the current match)
            a. If $distVector([L_i, L_j], [K_i, K_j]) < threshold\ \varepsilon$
               i. Store couple (L_i, K_i) and (L_j, K_j) in $mMatch$, increase $nCouple$ by 1
               ii. If $(nCouple > 4)$, set $mResult = 1$, go to step 4
               iii. Else go to step 2.c.i
            b. End
         3. End
      ii. End
   d. End
3. End
4. If $(mResult == 1)$
   a. Compute the affine transformation AF from stored couple in $mMatch$
   b. Using the transformation AF, compute the transformed position P_i for each spacecrafts landmarks L_i. A landmark in the geo-referenced image is a match of L_i if and only if their difference in position is smaller than ε.
5. Else report Failure

Figures 5 shows two examples of the found landmarks matches with different illumination conditions. The geo-referenced image (left side) is acquired with 55-25 (azimuth-elevation) sun position whereas the spacecraft images (right side) are acquired at 5710m altitude with 145-10 Sun angle (figure 5.a) and at 3052m altitude with 235-10 Sun angle (figure 5.b). The center images show the corresponding match region of the right-side images in the geo-referenced image. The spacecraft images are rotated for comparison purpose.

IV. RESULTS

IV.A. Spacecraft Position Estimation

Given a set of matches between the landing image and the geo-referenced image, the spacecraft position can be estimated by using:

1. The landmarks 2D positions (U) in the landing image
2. The landmarks 3D positions (M) in the landing zone (deduced through their matches with the geo-referenced image) expressed in a known coordinates
3. The image projection function:

$$U = K[R, -RT]M \tag{6}$$

where K is the 3×3 intrinsic matrix of the camera, R the image rotation (provided by the navigation filter) and T the s/c position (figure 6). For simplification purpose, the spacecraft reference frame is assimilated to the camera one here.

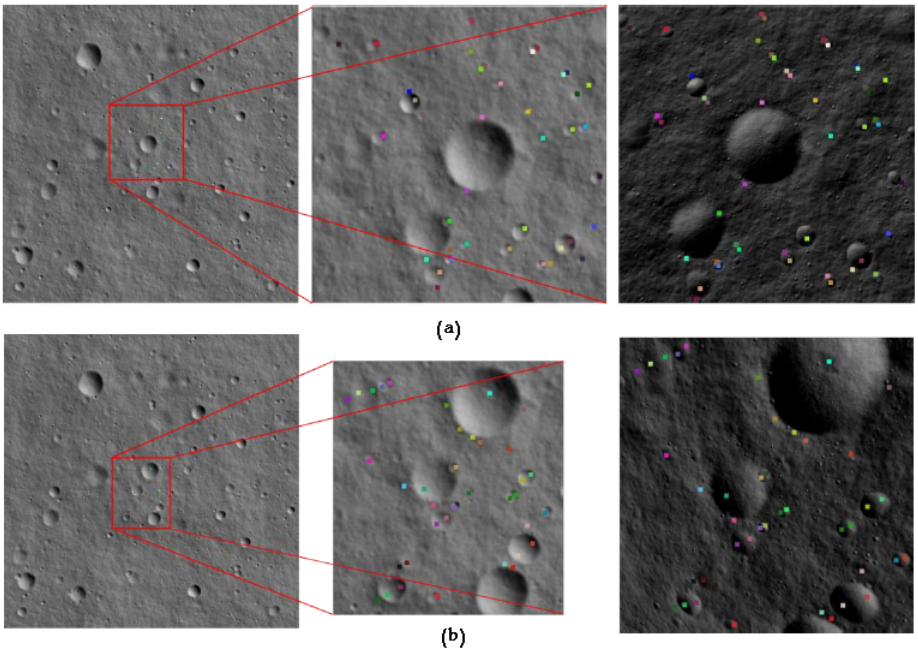

Figure 5. Matches with different illumination conditions (a) First example (b)Second example

Knowing U, K, R and M, the spacecraft position T can be calculated using a linear or non-linear optimization algorithm (e.g. Levenberg-Marquardt).

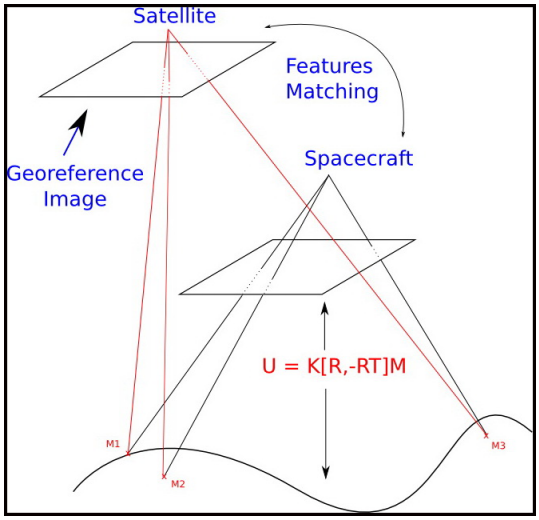

Figure 6. Spacecraft Position Estimation Principle

IV.B. Absolute position estimation results

The Landstel landmarks matching algorithm has been tested with the PANGU simulator v2.7. In this experiment, instead of using a simulated trajectory of a spacecraft during its entry phase (from the early parachute phase to the end of powered guidance phase), images are independently taken from $5000m$ altitude down to $1000m$ altitude. Each image is independently matched with the geo-referenced image, using the altitude and attitude information provided by the navigation filter as an input the resulting absolute position estimates are the core output of Landstel, and are not further fused by the navigation filter.

The purpose of this experiment, on one hand, is to verify the robustness of the Landstel system with different altitudes. On the other hand, the experiment shows how to choose the corresponding geo-referenced image with respect to the spacecrafts altitude considering the scale robustness. In reality, one very high resolution image can hardly match with a coarse image. Therefore depending on the landing images resolution, a corresponding geo-referenced image will be chosen for the matching step.

More precisely, there are two geo-referenced images used in this experiment. These two geo-referenced images form a two-layered image pyramid. In fact, an image pyramid may have more layers depending on the resolution of the lowest layer. In this experiment, the first one is taken at $182280m$ altitude with a camera of 10 degrees FOV and 2048×2048 pixels. The second one is also taken at $182880m$ altitude with a 5 degrees FOV camera and 2048×2048 pixels, which gives a two times finer resolution. Two corresponding landing image sets (68 images for each set) have been generated with PANGU to be matched with these geo-referenced images. The first series is taken from $5000m$ to $3000m$ and is matched with the first geo-referenced image; the second is taken from $2500m$ to $1050m$ and matched with the second geo-referenced image.

In order to verify the robustness of the system with different noise sources like illumination difference, camera noise, and sensor noise, the experiment is set up with the following configuration:

1. *Image illumination:*
   (a) *Geo-referenced image:* 55 *deg in azimuth,* 25 *deg in elevation (sun)*
   (b) *Landing image:* 40 *deg in azimuth,* 20 *deg in elevation (sun)*
2. *Image noise: white noise* $(0, 0.007)$
3. *Sensor noise:*
   (a) *Radar altimeter: 2.5 percents of measured distance (e.g.* $5000m$ *altitude with* $\pm 125m$ *error)*
   (b) *Gyroscope: error in margin* ± 5 *degrees*

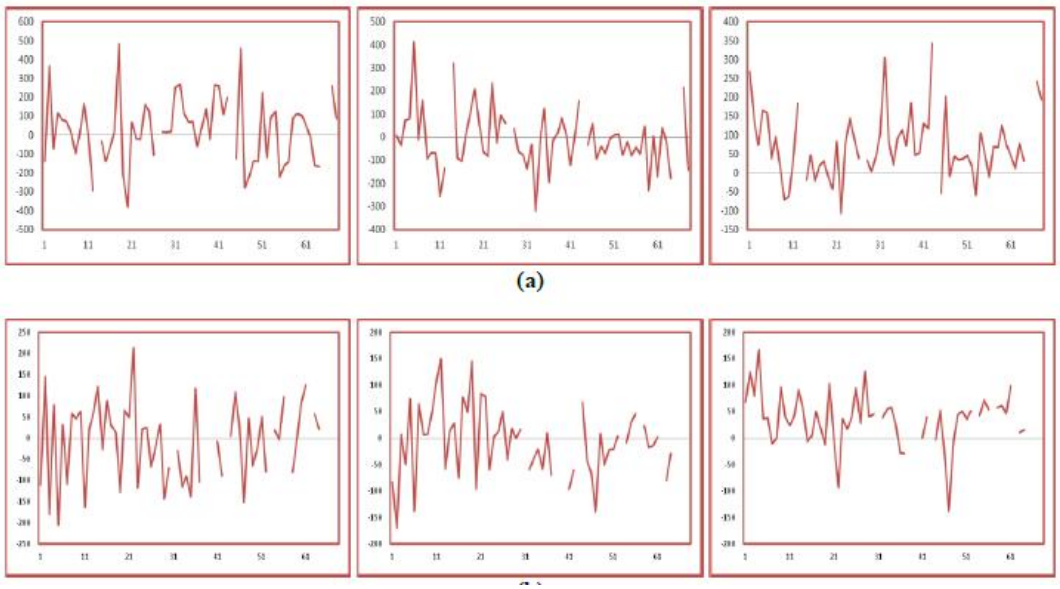

Figure 7. Landstel Result (a) 1st series 5000-3200m (b) 2nd series 2500 1050m. The horizontal axis denotes image series number from 1 to 68 whereas the vertical axis denotes difference between estimated position value and ground truth. The left, middle and right images respectively show difference in X, Y, and Z spaceraft's position with ground truth.

Results of absolute position estimates are shown in figure 7. The difference between the estimated values (X, Y, Z) and the true spacecraft position (ground truth) is calculated for each image. Errors in X, Y and Z are respectively displayed in the left, center and right columns. Figure 7.a shows the result of the first

image series (5000-3200m). Figure 7.b shows the result of the second image series (2400-1050m). The gaps presented in the charts mean that (1) there are no correct matches found or (2) the estimated position is not consistent with the previous estimation or with the radar altimeter estimate.

Results of other test cases where the geo-referenced image sun's direction is fixed to 55-25 azimuth-elevation and where landing image sun's direction varies are shown in figure 8. The numbers in each cell shows the corresponding result of the associated landing image sun's azimuth-elevation test case. In each cell, the first number shows the average difference of the estimated position and the ground truth whereas the second number reveals the standard deviation of each case. The third one shows the total number of images where the Landstel system can find consistent matches and give consistent results (with respect to previous results to the radar altimeter estimate).

Azi\Ele	15	20	25	30	35
45		(202.96 ; 110.38 ; 57)	(213.80 ; 118.69 ; 54)	(189.54 ; 109.67 ; 45)	
50		(192.93 ; 111.31 ; 54)	(198.18 ; 98.93 ; 58)	(192.70 ; 104.44; 49)	
55	(185.83 ; 106 ; 60)		(209.79 ; 86.84 ; 43)		(194.09 ; 105.99 ; 47)
60		(189.96 ; 109.29 ; 63)	(177.73 ; 102.90 ; 58)	(183.18 ; 107.07 ; 55)	
65		(181.81 ; 95.44 ; 61)	(198.64 ; 156.48 ; 57)	(180.95 ; 108.01 ; 52)	

(a)

Azi\Ele	15	20	25	30	35
45		(103.66 ; 51.47 ; 69)	(101.19 ; 54.36 ; 57)	(91.33 ; 50.7 ; 61)	
50		(107.98 ; 83.24 ; 62)	(98.52 ; 54.08 ; 60)	(94.28 ; 49.24 ; 60)	
55	(107.2 ; 62.23 ; 63		(101.12 ; 53.55 ; 67)		(90.03 ; 51.01 ; 51
60		(99.38 ; 50.33 ; 62)	(97.65 ; 47.49 ; 61)	(103.17 ; 79.34 ; 60)	
65		(99.11 ; 51.90 ; 61)	(108.49 ; 71.73 ; 63)	(102.52 ; 73.02 ; 56)	

(b)

Figure 8. Other Landstel Results (a) 1st series 5000-3200m (b) 2nd series 2500 1050m. Horizontal and vertical axes respectively denote sun angle's elevation and azimuth values for each test case. The first number in each cell means average difference value (mean) whereas the second denotes the standard deviation value. The third number signifies the number of images where the Landstel algorithm can find consistent matches.

V. DISCUSSION

The proposed landmark matching approach shows to be robust to different sources of error like illumination, camera noise or sensor noise of experiments. From a huge uncertainty in the spacecraft position (32000m), the system can localize the spacecraft within a much smaller uncertainty $\pm 400m$ for the 1st series and $\pm 200m$ for the 2nd series. As shown in figure 7.a or in figure 7.b, the estimation error does not significantly reduce with the altitude. The reason for this phenomenon is that all images in the first (or in the second) series, are matched with the same geo-referenced image. More precisely, the image taken at 5000m and that taken at 3200m are all matched with the first geo-referenced image, whose resolution is approximate 15.6m/pixel, which is equal to the resolution of a spacecraft image taken at 5700m. In fact, the latter images in the series are harder to match with the geo-referenced image than the early images. The reason is that the further the spacecraft descends, the bigger the difference between the spacecraft image and the orbiter image is. The estimation error is, as a consequence, reduced in the second series when all images are matched with a more precise geo-referenced image, 7.8m/pixel in resolution. Consistent to the result displayed in figure 7, the results displayed in figure 8 also shows that the precision in the second image series where the geo-referenced image is twice better than that in the first series is also twice better

(both in term of average difference and of standard deviation). That means that if a finer geo-referenced image is used, the estimated position is promised to be better.

As shown in figure 5 and generally in figure 8, the Landstel system is robust with respect to very different illumination conditions between the spacecrafts image and the orbiters one. This illumination robustness is obtained thanks to the use of a landmark signature solely computed on the basis of geometric relations instead of radiometric information.

The Landstel system is also efficient in memory usage. In fact, for each landmark in the geo-referenced image, the system only needs 72 bytes for the signature, 3 float numbers (4 bytes for each) for the points 3D position and 2 integer numbers (4 bytes for each) of the point's 2D position. Therefore, with 2000 points for the first geo-referenced image, the system only requires 180 Kb. This number can even be lowered if the landmark position is appropriately quantized. This low memory requirement is a big advantage for the system in the case of spatial application where memory capability is limited.

VI. CONCLUSION

In this paper, we have introduced a vision-based algorithm for spacecraft localization. In the first step, the algorithm uses a scale adjustment operator to detect the correct scaled features which are visible when viewing from high altitude. Then, the geometric relationship between one landmark with its neighbors is used to establish its signature. Hamming distance between the spacecrafts landmarks signature with that of geo-referenced image is used to filter possible matches, which results in multiple hypothesis matches. The algorithm, by using vector distance of landmark couples, can then discard incorrect matches. Finally, an affine transformation between these correct matches is calculated. Further matches are found thanks to the computed affine transformation.

The algorithm , through the experiment setup, has shown its robustness to different sources of noise thanks to the use of geometric features. Moreover, the proposed algorithm is also efficient in term of memory usage. It only requires less than 1 Mb to store the whole $30km \times 30km$ landing zone information. The Landstel system also shows its simplicity in algorithm description, which gives an easiness for hardware implementation.

In the future, the Landstel algorithm will be tested with different kind of simulated surfaces (craters, sand dunes, roughness...) and also with real aerial/spatial images to verify its robustness. Furthure improvement can be made within landmark's signature or landmarks database management. Information fusion with other sources like IMU or NPAL camera[1] via a global navigation filter to enhance estimation result is also considered.

ACKNOWLEDGMENTS

This work is financially and technically supported by ESA and by EADS-ASTRIUM.

References

[1]EADS ASTRIUM, Galileo Avionica, University of Dundee, INETI, and SCISYS. Navigation for planetary approach & landing. *ESA Contract*, 2006.

[2]S. Belongie and J. Malik. Matching with shape context. *IEEE Workshop on Context Based Access of Image and Video Libraries*, 2000.

[3]Yang Cheng and Adnan Ansar. Landmark based position estimation for pinpoint landing on mars. *Proceedings of the 2005 IEEE International Conference on Robotics and Automation*, pages 1573 – 1578, 2005.

[4]Yves Dufournaud, Cordelia Schmid, and Radu Horaud. Image matching with scale adjustment. *INRIA Report*, 2002.

[5]Jean-Francois Hamel, David Neveu, and Jean de Lafontaine. Feature matching navigation techniques for lidar-based planetary exploration. *AIAA Guidance, Navigation and Control Conference and Exhibit*, 2006.

[6]C. Harris and M. Stephens. A combined corner and edge detector. *Proceedings of the 4th Alvey Vision Conference*, 1988.

[7]Andrew E. Johnson and James F. Montgomery. Overview of terrain relative navigation approaches for precise lunar landing. *IEEE Aerospace Conference*, 2008.

[8]David Lowe. Object recognition from local scale-invariant features. *ICCV*, 1999.

[9]S.M Parkes, I. Martin, M. Dunstan, and D. Matthews. Planet surface simulation with pangu. *SpaceOps*, 2004.

[10]E. Silani and M. Lovera. Star identification algorithms: Novel approach & comparision study. *IEEE Aerospace Conference*, 2006.

[11]Nikolas Trawny, Anastasios I. Mourikis, and Stergios I. Roumeliotis. Coupled vision and inertial navigation for pin-point landing. *NASA Science Technology Conference*, 2007.

[12]Nikolas Trawny, Anastasios I. Mourikis, Stergios I. Roumeliotis, Andrew E. Johnson, and James Montgomery. Vision-aided inertial navigation for pin-point landing using observations for mapped landmarks. *Journal of Fields Robotics*, 2006.

[13]Aron A. Wolf, Claude Graves, Richard Powell, and Wyatt Johnson. Systems for pinpoint landing at mars. *14th AIAA/AAS Space Flight Mechanics Meeting*, 2004.